

IMPACT OF A SURFACTANT ON FILM FLOW AND CRYSTALLIZATION FOULING IN FALLING FILM EVAPORATORS

M. Waack¹, S. Nied² and *H. Glade¹

¹ University of Bremen, Engineering Thermodynamics, Badgasteiner Str. 1, 28359 Bremen, Germany,
email: heike.glade@uni-bremen.de

² BASF SE, 67056 Ludwigshafen, Germany

ABSTRACT

Crystallization fouling is a major problem in thermal seawater desalination plants. A widely applied thermal desalination technology is multiple-effect distillation commonly using horizontal tube falling film evaporators. Crystallization fouling on the evaporator tubes strongly depends on film flow characteristics. The thickness of the liquid film on a horizontal tube was measured with an optical micrometer using light-emitting diode technology. Furthermore, scale formation was studied with artificial seawater in a horizontal tube falling film evaporator at pilot plant scale. The effects of a polyoxyalkylene triblock copolymer surfactant at various concentrations on falling film flow and scale formation were investigated. Scale mass and scale layer thickness were reduced in the presence of the surfactant in the falling film evaporator. The reduction of scale formation can be explained by a higher mass transfer resistance of the scale-forming salt ions toward the tube surface as a consequence of a thicker seawater film and damped surface waves in the presence of the surfactant.

INTRODUCTION

Horizontal tube falling film evaporators are commonly used in multiple-effect distillation (MED) plants for seawater desalination. Seawater is distributed onto the upper tube rows of a horizontal tube bundle by spray nozzles or by perforated plates. The liquid forms a thin film on the outside of the tubes and flows downward by gravity.

The liquid load can be characterized by the wetting rate. In the following, the wetting rate Γ is defined as the mass flow rate \dot{m} on both sides of the tube per unit tube length L :

$$\Gamma = \frac{\dot{m}}{L} \quad (1)$$

The film Reynolds number Re_F which describes the falling film flow is expressed as

$$Re_F = \frac{2\Gamma}{\mu} \quad (2)$$

with the wetting rate as defined in Eq. (1) and the dynamic viscosity μ of the liquid.

In falling film evaporators for seawater desalination, the initial wetting rate on the upper tube row commonly ranges between 0.06 kg/(s m) and 0.14 kg/(s m) [1], which corresponds to a film Reynolds number between 250 and 600 for a seawater temperature of 65 °C and a salinity of 35 g/kg.

Seawater is a multi-component salt solution, containing inversely soluble salts such as calcium carbonate, calcium sulfate and magnesium hydroxide [2]. As the seawater is heated, the solubility of these salts decreases and precipitation of supersaturated salts, mainly calcium carbonate and magnesium hydroxide, preferably starts on the heat transfer surface, forming a scale layer which deteriorates the heat transfer performance [3].

A thin seawater film at the outside of the tubes is favorable for a high heat transfer coefficient. However, lowering the liquid load and, consequently, reducing the liquid film thickness increase the threat of film breakdown, which may accelerate the precipitation of salts on the heat transfer surface and lowers the effective heat transfer area.

Falling film flow and crystallization fouling are crucial aspects to be considered in the design and operation of falling film evaporators. It is of utmost importance that the horizontal tubes are completely covered by a liquid film at all operating conditions. Mass transfer of the salt ions toward the heat transfer surface, scale removal rates as well as heat transfer are governed by the fluid dynamics [4]. However, the effects of film flow on crystallization fouling in falling film evaporators for seawater desalination have only scarcely been investigated [5].

Film flow can be strongly affected by surface-active substances which are referred to as surfactants in the following. Surfactants adsorb onto the interfaces resulting in a reduced surface and interfacial tension, thus, affecting tube wetting and film flow. Liquid droplet and jet formation highly depend on interfacial phenomena because the surface tension determines the capillary pressure which governs the onset of instability and, therefore, droplet detachment and jet breakup [6]. Several studies have shown that surfactants stabilize the liquid filament detaching from

the bottom of a horizontal surface [6 - 9]. On the one hand, the surfactant decreases the surface tension. On the other hand, surfactant concentration gradients at the interface lead to Marangoni stresses hemming the thinning of the liquid filament [6]. Moreover, the wave motion of the free-surface of a liquid film on a solid substrate is known to be affected by the presence of surfactants [10]. Various theoretical studies have shown a damping effect of surfactants on wave formation [11 - 13]. Some studies have revealed circumstances under which destabilizing effects may occur [14 - 16]. However, the impact of surfactants on film flow and scale formation on horizontal tubes has not been investigated in detail [17].

Recently, the effects of so-called wetting agents on the wetting behavior of different tube materials were studied by Glade et al. [17] in a falling film evaporator test rig. An enhancement of the wettability was proven even at a low concentration of 1 mg/L. Furthermore, the impact of a wetting agent on scale formation was examined for a very low liquid load, which usually provokes film breakdown. The scale was considerably reduced with the use of the wetting agent.

In a previous study by Waack et al. [18, 19], film flow and scale formation were investigated for various wetting rates with and without surfactant. Calcium-containing scale mass and scale layer thickness increase with decreasing wetting rate. Assuming diffusion-controlled calcium carbonate crystallization in the laminar-wavy falling film, increasing scale formation can be explained by an intensified mass transfer due to thinner liquid films and wave motion. As the mean film thickness increases and surface waves are mostly damped in presence of the surfactant, the mass transfer resistance is higher and, thus, scale formation is lower.

The objective of this study is to give further insights into falling film flow on horizontal tubes under the influence of a surfactant and its impact on crystallization fouling in falling film evaporators for seawater desalination. In this study, the focus is laid on the effects of the surfactant concentration and the ionic strength. Furthermore, the study shall contribute to better understanding whether the effects of the surfactant on scale formation can be attributed to its impact on falling film flow or to its adsorption on the liquid/solid interface and alteration of the substrate surface properties.

EXPERIMENTAL

Experiments were performed in two test rigs in order to closely analyze film flow characteristics on horizontal tubes on the one hand and to investigate their effects on scale formation under realistic process conditions on the other hand.

Materials

Surfactant. The influence of a polyoxyalkylene triblock copolymer surfactant was examined. Non-

ionic triblock copolymer surfactants consisting of hydrophilic poly(ethylene oxide), referred to as PEO, and hydrophobic poly(propylene oxide), referred to as PPO, in the form of either PEO-PPO-PEO or PPO-PEO-PPO were commercialized by BASF [20] under the tradename Pluronic® and are widely applied. Their properties depend on the size and the arrangement of their hydrophilic and hydrophobic portion. These triblock copolymers offer a unique possibility to easily modify the hydrophobic and hydrophilic properties by adding a desired number of subunits to the specific chain [21]. In the current study, the surfactant Pluronic® 31R1 of the type PPO-PEO-PPO, referred to as 31R1, was used. It has a hydrophilic portion of 10 % and a rather low average molecular weight of 3250 g/mol. The cloud point (with 1 wt.%) is at 25 °C indicating phase separation [20]. The surfactant 31R1 offers a high surface activity and good wetting properties [20].

In the following, the concentration of the surfactant is given in ppm, which refers to milligrams of surfactant per kilograms of solution. The mass of the surfactant was determined with a semi-micro scale (AJ100, Mettler-Toledo, Germany) with an accuracy of ± 0.0001 g.

Test solutions. Film thickness measurements were performed using deionized (DI) water or sodium chloride (NaCl) solutions with different ionic strengths between 0.72 and 5.30 mol/kg_{solvent} in order to study the effect of dissolved electrolytes on the film flow and the surface activity of the surfactant without provoking scale formation. The chosen ionic strengths equal those of artificial seawater with a salinity between 35 g/kg and 210 g/kg.

For the scaling experiments, artificial seawater based on salt mole fractions for standard artificial seawater as suggested in the formulation by Kester et al. [22] was used. The composition of artificial seawater is within 1 mg/kg of natural seawater for all the major constituents [22]. Artificial seawater with a high salinity of 65 g/kg and an ionic strength of 1.39 mol/kg was chosen, representing concentrated brine at the bottom of an MED tube bundle. The initial pH value was approximately 8.3 which is similar to pH values in industrial multiple-effect distillers [23].

Tubes. Aluminum brass tubes (CW 702 R) with an outer diameter of 25 mm and a wall thickness of 1 mm were used in the tests. The tube material and dimensions are widely applied in MED plants. The tubes were used with their typical surface topography as delivered by the tube supplier (MPG Mendener Präzisionsrohr GmbH (Germany)) with a mean surface roughness of 0.73 μm . The tubes were thoroughly cleaned with isopropyl alcohol and acetone before each experiment.

Film flow measurements

In the following, the film thickness test rig and the experimental procedure are described.

Test rig. A unique test rig was constructed for the investigation of the film flow on horizontal tubes, comprising a bank of four tubes and a high-resolution optical micrometer, as illustrated in Fig. 1. The test liquid is evenly distributed onto a bank of four horizontal tubes arranged one below the other. A perforated transparent polymer tube with liquid supply at both ends serves as liquid distribution system. The distribution tube has an outer diameter of 16 mm and a wall thickness of 2 mm. Holes with a diameter of 1 mm are aligned with a distance of 5 mm on the bottom of the tube. The center of the distribution tube is positioned 50.5 mm above the center of the first tube. The first two tubes of the test section serve to homogenize the liquid flow. The wetted length of the tubes is 300 mm. The vertical distance of the tube centers is 62 mm. The tubes are not heated.

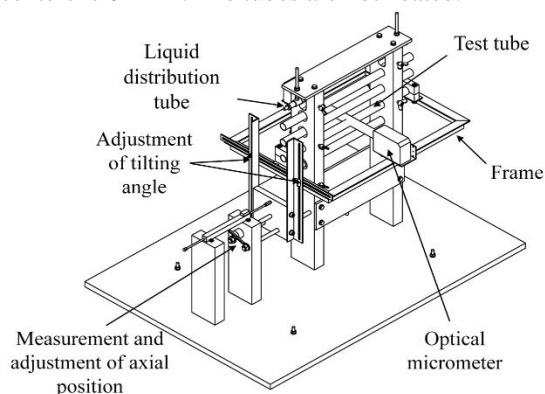


Fig. 1: Film thickness test rig with optical micrometer

A centrifugal pump conveys the test liquid from a feed tank through a heating coil placed in a thermostat bath to the liquid distribution tube at the top of the test section. The volume flow rate of the test liquid is controlled by a needle valve. Before the test liquid enters the distribution tube, its temperature is measured by a Pt100 temperature sensor (accuracy class A) and its volume flow rate is measured by a turbine flow meter (FCH-midi-PVDF, Biotech, Germany). The flow meter exhibits a measuring accuracy of $\pm 2\%$.

The liquid film thickness is measured on the third tube by means of an optical micrometer (optoCONTROL 2600, Micro-Epsilon, Germany) at a high sampling rate. The micrometer uses light-emitting diode (LED) technology and exhibits a resolution of $0.1 \mu\text{m}$, a reproducibility of $\pm 1 \mu\text{m}$ and a linearity of $\pm 3 \mu\text{m}$.

The optical micrometer is mounted on a steel frame which, in turn, is directly fixed on the test tube avoiding the measurement of vibrations and thermal expansion. The frame can be moved in axial direction of the tube as well as around the tube. The axial position is measured by means of a potentiometric position sensor (FWA150T, Ahlborn, Germany) with a measuring accuracy of $\pm 0.01 \text{ mm}$. The tilting angle is determined by means of a digital protractor with a measuring accuracy of $\pm 0.1^\circ$.

Test procedure. Film thickness measurements were performed using DI water without surfactant and with a surfactant concentration ranging from 5 ppm to 100 ppm at a wetting rate of $0.04 \text{ kg}/(\text{s m})$ and a water temperature of 65°C ($Re_F = 184.6$, laminar-wavy regime). In another test series, the effects of the ionic strength of a NaCl solution on the film flow without surfactant and with a surfactant concentration of 50 ppm were studied at a wetting rate of $0.04 \text{ kg}/(\text{s m})$ and 25°C .

Before each measurement, the surface of the third tube (test tube) was locally dried by compressed air and by covering the tube surface directly above the measuring spot along a length of around 3 cm. The film flow above the third tube was not affected by this procedure. The shaded length measured by the LED micrometer was set to zero for the dry tube surface. The blockage of the liquid distribution was removed afterwards. The measurement of the film thickness was started once the tube surface was completely rewetted.

The film thickness was measured on the top and on the bottom of the third tube, referred to as 0° and 180° , respectively, along an axial length of 90 mm. Measurements were performed 45 mm left and right from the middle of the tube length at 19 measuring points at a distance of 5 mm whereas the middle of the tube length is located at a position of $x = 150 \text{ mm}$. Moreover, the film thickness was measured at circumferential angles φ between 0° and 180° at three different axial positions, namely the middle of the tube length as well as 20 mm left and right from the middle. Measurements could only be performed from 0° to 50° as well as from 130° to 140° as the LED light curtain is blocked by the other tubes at high tilting angles of the steel frame and by pendant liquid on the tube bottom at high circumferential angles. At each measuring point, the film thickness was recorded for 5 min at a sampling frequency of 230 Hz.

Test evaluation. Owing to the dynamic nature of the liquid film, a wide range of film thicknesses was recorded at each measuring point. Therefore, statistical evaluation of the data was necessary. The mean film thickness and the mean minimum film thickness were determined. The surface of the falling liquid film is in wavy motion. In order to analyze the wave motion, the power spectrum was estimated by means of the Welch's method [24]. The highest peak in the power spectrum is related to the maximum amplitude at the dominant frequency. The signal-to-noise ratio was always higher than 50 dB for each measurement. Data evaluation is described in detail by Waack et al. [19].

Scaling experiments

In the following, the falling film evaporator test rig and the experimental procedure are described.

Test rig. Scaling experiments were performed in a falling film evaporator test rig at pilot plant scale. The main component of the test rig is an evaporator equipped with a bank of six horizontal tubes arranged one below the other. The tubes are attached to the tube

sheets with screws and they are sealed by means of O-rings. The tube length which is wetted by seawater amounts to 453 mm. The vertical distance between the tube centers is 50 mm. Seawater is evenly distributed onto the first tube by a toothed overflow weir. Inspection glasses on both sides of the evaporator shell allow a visual observation of the film flow.

The tubes are heated from the inside by heating steam, which is generated by an electrical steam generator. The heating steam condenses inside the tubes and the condensate is directed back to the steam generator. Heat is transferred from the steam inside of the tubes to the seawater on the outside of the tubes. The seawater forms a thin film on the outer tube surface. It is first preheated up to saturation temperature on part of the first tube and then partially evaporates on the subsequent tubes. Evaporation takes place at a pressure below ambient pressure, which is maintained by a vacuum pump. The generated vapor is directed to a condenser and the condensate is collected in a tank equipped with a level indicator. After leaving the evaporator, the concentrated seawater flows into a collecting tank where it is mixed with the distillate in order to keep the salinity of the seawater approximately constant. The seawater is conveyed back to the evaporator by a centrifugal pump. Various temperature, pressure and flow sensors are implemented in the test rig in order to monitor and control the process conditions.

Test procedure. The surface free energy of aluminum brass tubes which were immersed in DI water without any surfactant and in DI water with 50 ppm of the surfactant 31R1 for 1 h at a temperature of 23 °C was determined by contact angle measurements using a drop shape analyzer (DSA, KRÜSS GmbH, Germany). Three different test liquids were used, namely water, diiodo-methane and ethylene glycol. Measurements were carried out at least eight times on different spots of the respective tube.

Scaling tests were performed using artificial seawater without surfactant and with a surfactant concentration ranging from 5 ppm to 100 ppm.

In another test series, the tube surfaces were treated with the surfactant prior to the tests. The tubes were immersed in 15 liters of an aqueous solution of the surfactant 31R1 with a concentration of 1000 ppm for 24 h. A high concentration of 1000 ppm was chosen in order to reduce the adsorption time. Then experiments were performed without dosing a surfactant to the artificial seawater.

In all scaling tests, an evaporation temperature of 65 °C in the evaporator shell and a condensation temperature of 70 °C inside the tubes were chosen, representing common conditions in the first stage of an MED plant. Tests were performed at a wetting rate of 0.04 kg/(s m) ($Re_F = 157.1$). In falling film evaporators, wetting rates can easily fall below the initial value due to evaporation and liquid maldistribution. Therefore, a low value of 0.04 kg/(s m) was chosen.

Experiments with 240 liters of artificial seawater and time periods of 50 hours were found to be favorable because time periods are long enough to find differences in scale formation and supersaturation levels are still high enough.

The evaporator was dismantled after each test run. Tubes were carefully removed. The inside of the evaporator was manually cleaned with DI water and with diluted acetic acid solution. The collecting tank for seawater was cleaned with water jets. In addition to that, the evaporator was cleaned with a 20 vol.% isopropyl alcohol solution recirculating for a minimum of 2 h. Subsequently, the whole circuit was cleaned by flushing with DI water for several days.

Test evaluation. The scale layer thickness was measured by means of a gauge (MiniTest 2100, ElektroPhysik, Germany) in combination with the probe FN 1.6 using the eddy current method. The measuring range of the probe is between 0 µm and 1600 µm. It exhibits a high resolution of 0.1 µm. The tolerance amounts to ±1 µm due to the calibration standard. A two-point calibration was performed at each tube. First, the probe was placed on a clean sample determining the lower reference value. Then a calibration foil with a thickness of 96 µm (± 1 µm) was used. The scale layer thickness was measured on each of the six evaporator tubes at four different circumferential angles, namely 0°, 90°, 180° and 270°. At each circumferential angle, the scale layer thickness was measured at 25 different points along the tube. The distance between the measuring points along the tube was 10 mm near to the tube center and 20 mm near to the ends of the scale layer. The scale layer edges at both tube ends were excluded from the measurements. The thickness was measured 10 times at each position.

Scale formation is dominated by calcium carbonate and magnesium hydroxide precipitation during seawater evaporation [25]. Therefore, the calcium and magnesium contents of the scale on the fourth evaporator tube were determined by inductively coupled plasma atomic emission spectroscopy (ICP-AES). The scale layers at the edges were removed with sandpaper along a length of 1 cm on each side before analysis in order to only determine the scale on the main tube body. The scaled tube was submerged in a 10 wt.% acetic acid solution at a temperature of 90 °C for 2 h in order to dissolve the scale.

RESULTS

In the following, the results of the film thickness measurements and scaling experiments are presented.

Film thickness and wave motion

Impact of the surfactant concentration. As shown in Fig. 2, the axial mean film thickness with a surfactant concentration of 5 ppm and 10 ppm is comparable to that of pure DI water at the tube top. It slightly increases at 50 ppm and 100 ppm where it is higher compared to that of pure DI water.

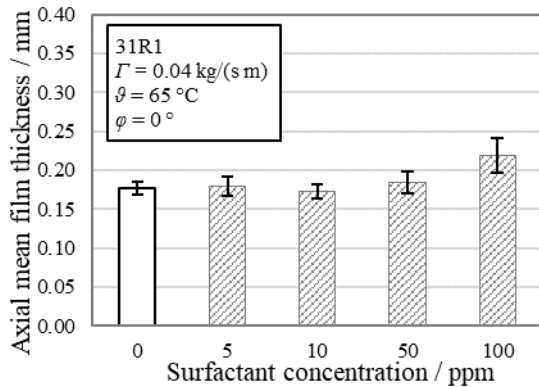


Fig. 2. Axial mean film thickness for different surfactant concentrations at the tube top.

The same trend of the axial mean film thickness can be observed with increasing surfactant concentration at the bottom of the tube, as shown in Fig. 3.

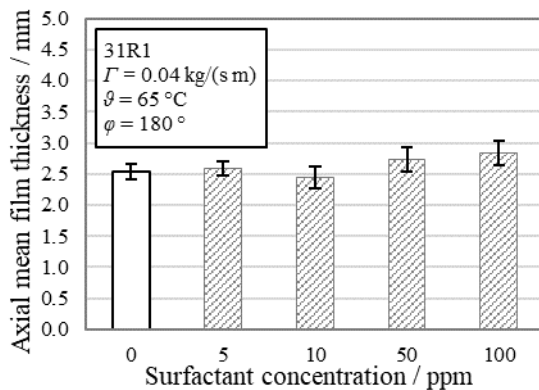


Fig. 3. Axial mean film thickness for different surfactant concentrations at the tube bottom.

The mean film thickness was also determined for different circumferential angles between 0° and 180° . On the upper half of the tube, surfactant concentrations of up to 50 ppm did not significantly affect the mean film thickness compared with that of pure DI water. However, a high concentration of 100 ppm notably increased the mean film thickness.

On the lower half of the tube, the mean film thickness of the 31R1 solutions exceeded the one of pure water except for a concentration of 5 ppm. Moreover, the mean film thickness appeared to increase with increasing surfactant concentration.

As shown in Fig. 4, the axial mean minimum film thickness significantly decreases with increasing surfactant concentration at the tube top. Similar to the tube top, the minimum film thickness measured between circumferential angles of 10° and 140° decreases with increasing surfactant concentration. On the upper half of the tube, even a minimum film thickness of zero was measured at high surfactant concentrations representing a dry tube surface.

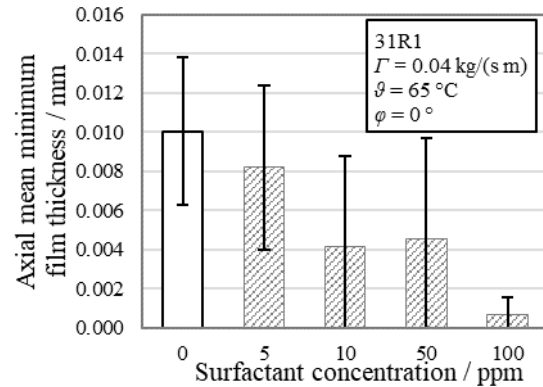


Fig. 4. Axial mean minimum film thickness for different surfactant concentrations at the tube top.

In contrast to the tube top, the axial mean minimum film thickness increases in the presence of the surfactant at the tube bottom compared with that of pure DI water, as shown in Fig. 5. It only slightly changes with the surfactant concentration.

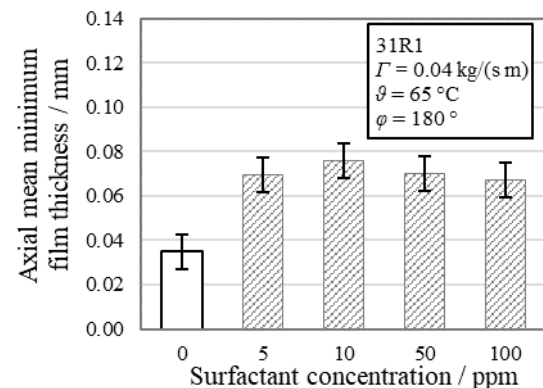


Fig. 5. Axial mean minimum film thickness for different surfactant concentrations at the tube bottom.

Figure 6 shows the maximum wave amplitude in the middle of the tube for various circumferential angles and different surfactant concentrations.

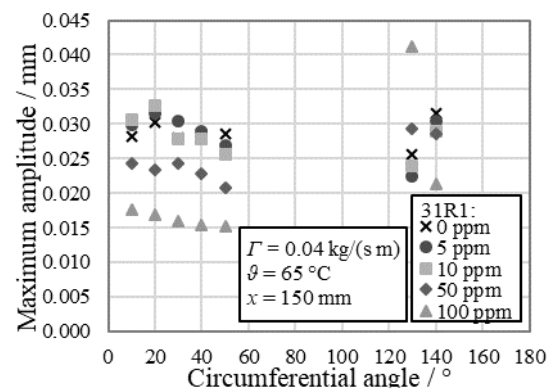


Fig. 6. Maximum wave amplitude in the middle of the tube in dependence of the circumferential angle for different surfactant concentrations.

As illustrated in Fig. 6, on the upper half of the tube, the maximum amplitude is significantly reduced

compared with that of pure DI water in case of high concentrations of 50 ppm and 100 ppm, which reflects the measured trend at the tube top. In contrast, the maximum amplitude of the 31R1 solutions is similar to that of pure DI water at circumferential angles of 130° and 140° except for the ones at a concentration of 100 ppm which show no clear trend.

Influence of the ionic strength. Experiments with NaCl solutions showed no significant effects of the ionic strength on the falling film characteristics without surfactant, as illustrated in Fig. 7.

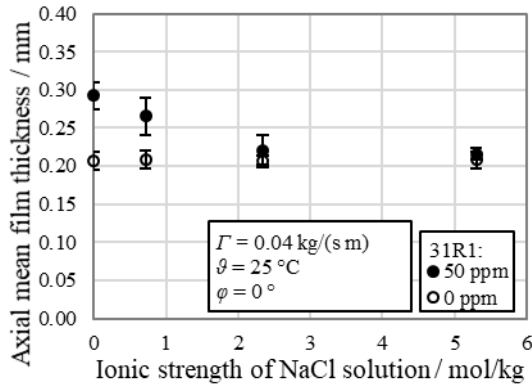


Fig. 7. Axial mean film thickness with and without surfactant depending on the ionic strength of the NaCl solution at the tube top at 25 °C.

However, the axial mean film thickness is higher with surfactant compared to that without surfactant at the tube top for low ionic strengths, as shown in Fig. 7. The film thickness of the surfactant solution gradually approaches the one without surfactant with increasing ionic strength.

In contrast, the ionic strength has no systematic influence on the axial mean film thickness with and without surfactant at the tube bottom, as shown in Fig. 8. The axial mean film thickness of the surfactant solution is similar to that without surfactant.

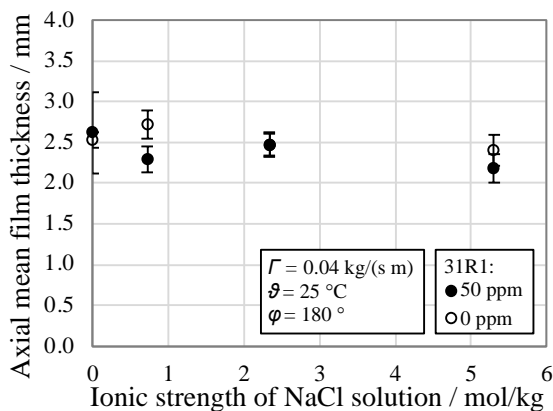


Fig. 8. Axial mean film thickness with and without surfactant depending on the ionic strength of the NaCl solution at the tube bottom at 25 °C.

Figure 9 illustrates the axial mean maximum wave amplitude at the tube top. In the absence of salt ions, the axial mean maximum amplitude is slightly higher with surfactant than without. It decreases with increasing ionic strength of the solution and falls significantly below the one without surfactant.

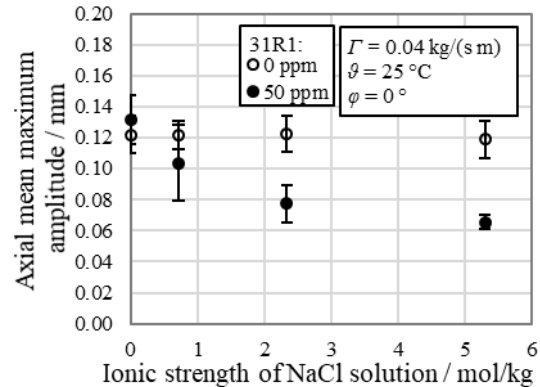


Fig. 9. Axial mean maximum wave amplitude with and without surfactant in dependence of the ionic strength of the NaCl solution at the tube top at 25 °C.

In contrast, the axial mean maximum amplitude at the tube bottom is higher with surfactant than without for each investigated ionic strength, as illustrated in Fig. 10. In case of the surfactant solution, it increases with increasing ionic strength at first but drops at the highest ionic strength.

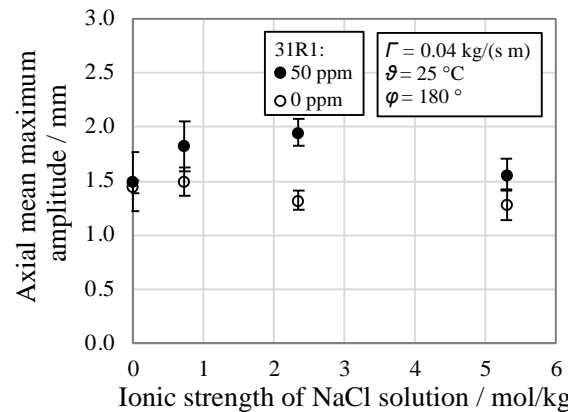


Fig. 10. Axial mean maximum wave amplitude with and without surfactant in dependence of the ionic strength of the NaCl solution at the tube bottom at 25 °C.

Scale formation during seawater evaporation

Impact of the surfactant concentration. The calcium scale masses per tube surface area on the fourth tube are illustrated in Fig. 11 for artificial seawater without and with various 31R1 concentrations.

The calcium scale mass per surface area is reduced in the presence of the surfactant except for a concentration of 10 ppm, as shown in Fig. 11. The reduction of the specific calcium mass is most significant at 5 ppm. In accordance with previous

results [25] without surfactant, the specific magnesium scale mass was two orders of magnitude lower than the specific calcium mass and amounted to 0.15 g/m². It was slightly reduced by the surfactant for concentrations below 100 ppm.

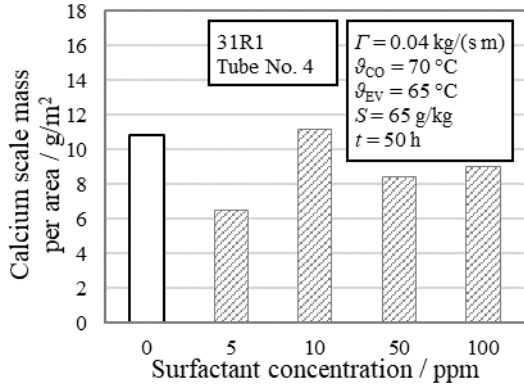


Fig. 11. Deposited calcium scale mass per tube surface area on the 4th tube for various 31R1 concentrations.

The axial mean scale layer thickness in the presence of the surfactant is lower than that without surfactant at each circumferential angle, as shown in Fig. 12. However, the scale-reducing effect of the surfactant is less pronounced at a concentration of 10 ppm. Similar to scale formation without surfactant, the strongest scale formation occurs at the tube sides (90° and 270°) followed by the tube top (0°) and the tube bottom (180°).

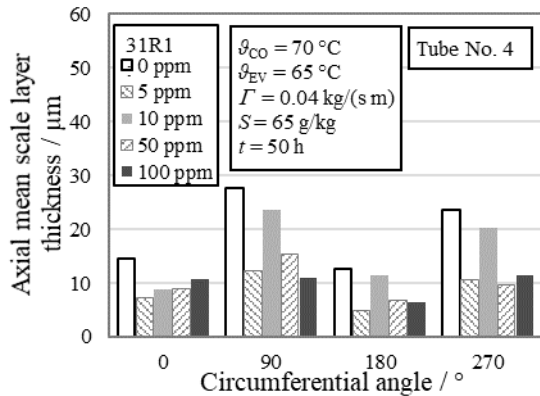


Fig. 12. Axial mean scale layer thickness on the 4th tube at different circumferential angles for various surfactant concentrations.

As shown in Fig. 13, the overall mean scale layer thickness is reduced on each of the six tubes in the presence of the surfactant.

However, the reducing effect of the surfactant is less pronounced at the concentration of 10 ppm on the tubes four to six. Similar to scale formation without any surfactant, the scale layer thickness increases from the upper tube to the lower tube in the presence of the surfactant, as shown in Fig. 13.

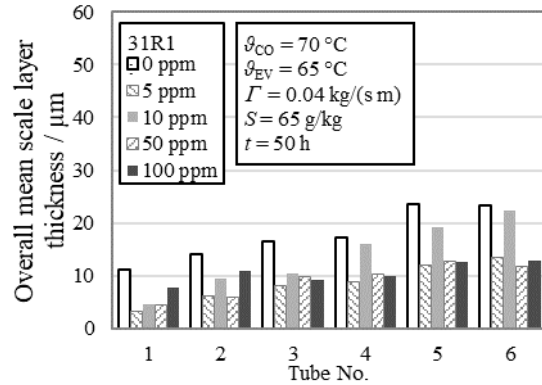


Fig. 13. Overall mean scale layer thickness on each evaporator tube for various surfactant concentrations.

Influence of surface pretreatment. In order to better understand whether the effects of the surfactant on scale formation can be attributed to its impact on falling film flow or to its adsorption on the liquid/solid interface and alteration of the substrate surface properties, the tube surfaces were pretreated.

The surface free energy of aluminum brass tubes which were immersed in DI water without any surfactant and in DI water with 50 ppm of the surfactant 31R1 for 1 h at a temperature of 23 °C was determined. As shown in Table 1, the 31R1 solution slightly increases the surface free energy of the substrate, especially the polar part of the surface energy increases.

Table 1. Surface free energy of aluminum brass tubes after immersion in DI water and in 31R1 solution (50 ppm) for 1 h at 23 °C.

		DI water	31R1
Surface free energy	mN/m	34.50 ± 4.35	37.61 ± 3.87
Dispersive part	mN/m	33.24 ± 3.66	33.99 ± 2.93
Polar part	mN/m	1.26 ± 0.7	3.62 ± 0.93

Prior to the scaling tests, the aluminum brass tubes were exposed to an aqueous solution of the surfactant 31R1 with a concentration of 1000 ppm for 24 h. Scaling tests were performed in the horizontal tube falling film evaporator afterwards without dosing a surfactant to the artificial seawater.

Figure 14 compares the calcium scale mass per tube surface area and the overall mean scale layer thickness for experiments without surfactant, with pretreated test tubes and with the 31R1 surfactant.

The calcium scale mass and the overall mean scale layer thickness on the pretreated tubes are similar to those on the untreated tubes. However, a surfactant concentration of 50 ppm in the seawater during the test leads to a notable reduction of the calcium scale mass and the scale layer thickness, as shown in Fig. 14.

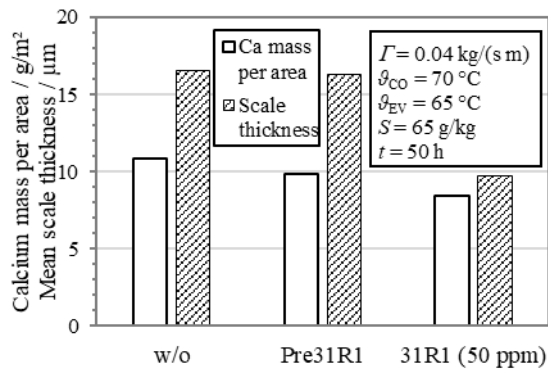


Fig. 14. Calcium scale mass per tube surface area (4th tube) and overall mean scale layer thickness (3rd tube) without surfactant, using tubes pretreated with 31R1 prior to the test and with use of 31R1 during the test.

DISCUSSION

The effects of film flow on scale formation are very complex because heat transfer as well as mass transfer are affected. Scale formation depends on mass transfer of involved species toward the surface and reaction rates. Moreover, precipitated salt crystals can be removed by shear forces. Experimental results without surfactant are described and discussed in more detail by Waack et al. [18].

Scale formation and film flow were studied in the presence of the surfactant 31R1 with a concentration ranging from 5 ppm to 100 ppm at a wetting rate of $0.04 \text{ kg}/(\text{s m})$. It should be noted that the cloud point of the 31R1 solution with a concentration between 5 ppm and 100 ppm was exceeded at the high temperature of $65 \text{ }^\circ\text{C}$. Phase separation limits the surface activity of the surfactant. However, the surfactant 31R1 still greatly affects the falling film flow on horizontal tubes.

Surfactants influence film flows in two ways: firstly, by lowering the surface tension, and secondly, as the surfactant concentration along the interface can be nonuniform, they cause the interface to be subjected to a surface tension gradient and, therefore, Marangoni stress opposing or promoting the local thinning of the liquid film [11 - 16, 21].

As depicted in Figs. 2 and 3, the mean film thickness of the 31R1 solutions is higher than or similar to that of pure water. Moreover, the maximum wave amplitude is damped on the major part of the tube circumference, as shown in Fig. 6. The free surface of a liquid is subjected to disturbances which lead to changes in the interfacial area. The surface concentration of the surfactant is locally reduced. Consequently, gradients of surface tension in lateral direction are induced by the surfactant concentration gradients [26]. The induced surface tension gradients lead to tangential stresses in the interface, which are also referred to as Marangoni stresses [27]. The tangential stresses give rise to a resistance against surface deformation resulting in a surface viscoelasticity [28]. The surface viscoelasticity results in the damping of the wave amplitude. The damping,

in turn, leads to the dissipation of kinetic energy. As the kinetic energy is reduced, the liquid is decelerated and the film thickness increases.

Assuming a diffusion-controlled crystallization of calcium carbonate in the laminar-wavy falling film under the examined process conditions, as explained by Waack et al. [18], both effects, the increased film thickness and the reduced wave amplitude, lead to a higher mass transfer resistance with regard to the scale-forming salt ions. Accordingly, scale formation on the tube surface is reduced.

The minimum film thickness is substantially lowered in the presence of the surfactant near the tube top, even temporarily down to zero, as illustrated in Fig. 4. A liquid film can also be destabilized by solutocapillary effects [14 - 16]. Higher evaporation rates of the solvent in the trough regions of the wavy film compared with that of the crest regions presumably lead to a locally high surfactant concentration and consequently to a Marangoni flow destabilizing the liquid film. A lower minimum film thickness would promote scale formation. However, film breakdown was not observed in the falling film evaporator test rig.

At the tube bottom, the minimum film thickness increases in the presence of the surfactant, as shown in Fig. 5. The wave damping effect of the surfactant is dominant. A higher minimum film thickness leads to a higher mass transfer resistance regarding the scale-forming ions and consequently a reduced scale formation. As depicted in Figs. 11 to 13, most scale formed at a 31R1 concentration of 10 ppm compared with that at other concentrations. The results suggest that the stabilization of the free-surface of the seawater film is less effective at this concentration. As shown in Figs. 2 and 3, a minimum of the mean film thickness at the tube top and the tube bottom for 10 ppm supports this assumption.

Liquid filaments detaching from the tube bottom are less effectively stabilized by the surfactant with increasing ionic strength. The solubility of the Pluronic[®] surfactants decreases once a salt is introduced into the system [29]. The addition of salts causes a dehydration of the PEO chain similar to the effect of an increasing temperature [29]. As the surface activity of the surfactant is reduced, the intertube flow pattern gradually changes from the jet regime to the droplet regime with increasing ionic strength. The axial mean film thickness at the tube top decreases and approaches that of the solution without surfactant, as shown in Fig. 7. Moreover, the damping effect of the surfactant on the dominant wave amplitude at the tube top is promoted by an increased ionic strength, as shown in Fig. 9. The diffusional transport of surfactant molecules from the solution to the interface is hemmed by the promoted tendency towards self-aggregation in presence of salt ions [30]. Consequently, the relaxation of surface tension gradients is slower which results in a higher surface viscoelasticity and therefore a stronger damping effect.

The surface energy of a tube pretreated with a 31R1 solution is higher compared with that of the untreated tube, as shown in Table 1, which may increase the fouling propensity. A higher surface energy may lead to stronger adhesion of the salt causing a shortened induction period and an increased scale formation [31, 32]. However, neither the scale layer thickness nor the calcium scale mass on pretreated tubes notably differ from the ones on untreated tubes, as shown in Fig. 14. Consequently, the adsorption of the surfactants onto the solid/liquid interface does not appear to notably affect scale formation. It should be noted that the pretreated tubes were in contact with artificial seawater without surfactant during the test. Consequently, the adsorbed surfactant presumably at least partially dissolved in the test solution causing a decrease of the surface energy.

CONCLUSIONS

Falling film flow on horizontal tubes and its impact on crystallization fouling during seawater evaporation were studied. Furthermore, the impact of the triblock copolymer surfactant Pluronic® 31R1 was investigated. The surfactant concentration was varied between 5 ppm and 100 ppm.

Film thickness and wave motion play an important role in scale formation. Scale mass and scale layer thickness are reduced in the presence of the surfactant in the falling film evaporator. The reduction of scale formation can be explained by a higher mass transfer resistance of the scale-forming salt ions toward the tube surface as a consequence of a thicker seawater film and damped surface waves in the presence of the surfactant. Experimental results with pretreated tube surfaces suggest that the reduction of scale formation in the presence of the surfactant can be mainly attributed to its effects on the falling film flow rather than to its adsorption onto the tube surface and the alteration of the tube surface properties.

Further studies with non-ionic and ionic surfactants should be performed to obtain a wider overview of the impact of the molecular structure on interfacial phenomena and scale formation. Scaling experiments should be carried out with varying seawater salinities and evaporation temperatures.

NOMENCLATURE

L	tube length, m
\dot{m}	mass flow rate, kg/s
Re_F	film Reynolds number, dimensionless
S	salinity, g/kg
t	time, h
x	axial position, mm
Γ	wetting rate, kg/(s m)
ϑ	temperature, °C
μ	dynamic viscosity, kg/(m s)
φ	circumferential angle, °

Subscript

CO	condensation
EV	evaporation

REFERENCES

- [1] Glade, H., Cetinkaya, S., Will, S., Nied, S., and Schürmann, G., Effects of the wetting rate on scale formation in multiple-effect distillers, *Proc. EuroMed*, Dead Sea, Jordan, Nov. 2008.
- [2] Millero, F. J., The composition of standard seawater and the definition of the reference-composition salinity scale, *Deep-Sea Research I*, vol. 55, no. 1, pp. 50-72, 2008.
- [3] Al-Anezi, K., and Hilal, N., Scale formation in desalination plants: Effect of carbon dioxide solubility, *Desalination*, vol. 204, no. 1-3, pp. 385-402, 2007.
- [4] Helalizadeh, A., Müller-Steinhagen, H., and Jamialahmadi, M., Mixed salt crystallisation fouling, *Chemical Engineering and Processing*, vol. 39, no. 1, pp. 29-43, 2000.
- [5] Stärk, A., Loisel, K., Odiot, K., Feßenbecker, A., Kempter, A., Nied, S., and Glade, H., Wetting behaviour of different tube materials and its influence on scale formation in multiple-effect distillers, *Desalination and Water Treatment*, vol. 55, no. 9, pp. 2502-2514, 2015.
- [6] Kovalchuk, N. M., Nowak, E., and Simmons, M. J. H., Effect of soluble surfactants on the kinetics of thinning of liquid bridges during drops formation and on size of satellite droplets, *Langmuir*, vol. 32, no. 20, pp. 5069-5077, 2016.
- [7] Kovalchuk, N. M., and Simmons, M. J. H., Effect of soluble surfactant on regime transitions at drop formation, *Colloids and Surfaces A: Physicochemical and Engineering Aspects*, vol. 545, pp. 1-7, 2018.
- [8] Timmermans, M. L. E., and Lister, J. R., The effect of surfactant on the stability of a liquid thread, *Journal of Fluid Mechanics*, vol. 459, pp. 289-306, 2002.
- [9] Craster, R. V., Matar, O. K., and Papageorgiou, D. T., Breakup of surfactant-laden jets above the critical micelle concentration, *Journal of Fluid Mechanics*, vol. 629, pp. 195-219, 2009.
- [10] Georgantaki, A., Vlachogiannis, M., and Bontozoglou, V., The effect of soluble surfactants on liquid film flow, *Journal of Physics: Conference Series*, vol. 395, no. 1, 012165, 2012.
- [11] Spivak, B., Vanden-Broeck, J.-M., and Miloh, T., Free-surface wave damping due to viscosity and surfactants, *European Journal of Mechanics-B/Fluids*, vol. 21, no. 2, pp. 207-224, 2002.
- [12] Ceniceros, H. D., The effects of surfactants on the formation and evolution of capillary waves, *Physics of Fluids*, vol. 15, no. 1, pp. 245-256, 2003.
- [13] Tomar, D. S., Baingne, M., and Sharma, G., Stability of gravity-driven free surface flow of surfactant-laden liquid film flowing down a flexible inclined plane, *Chemical Engineering Science*, vol. 165, pp. 216-228, 2017.

- [14] Blyth, M. G., and Pozrikidis, C., Effect of surfactant on the stability of film flow down an inclined plane, *Journal of Fluid Mechanics*, vol. 521, pp. 241-250, 2004.
- [15] Kim, K. J., Berman, N. S., and Wood, B. D., The interfacial turbulence in falling film absorption: Effects of additives, *International Journal of Refrigeration*, vol. 19, no. 5, pp. 322-330, 1996.
- [16] Gao, P., and Lu, X. Y., Effect of surfactants on the inertialess instability of a two-layer film flow, *Journal of Fluid Mechanics*, vol. 591, pp. 495-507, 2007.
- [17] Glade, H., Stärk, A., Sujandi, S., Loisel, K., Edwie, F., and Nied, S., Improvement of tube wetting by wetting agents in multiple-effect distillers, Proc. *IDA World Congress on Desalination and Water Reuse*, San Diego, USA, 2015.
- [18] Waack, M., Glade, H., and Nied, S., Falling film flow characteristics on horizontal tubes and their effects on scale formation in seawater evaporators, *Desalination and Water Treatment*, vol. 211, pp. 1-14, 2021.
- [19] Waack, M., Glade, H., and Nied, S., Effects of film flow and a surfactant on scale formation in falling film evaporators for seawater desalination, *Heat Transfer Engineering*, 2021, DOI: 10.1080/01457632.2021.1963090.
- [20] BASF Corporation, Surfactants: Pluronic® and Tetronic®, Printed brochure, Florham Park, NJ, USA, 2006.
- [21] Myers, D., Surfactant science and technology, vol. 3, John Wiley & Sons, Inc., Hoboken, NJ, USA, 2006.
- [22] Kester, D. R., Duedall, I. W., Connors, D. N., and Pytkowicz, R. M., Preparation of artificial seawater, *Limnology and Oceanography*, vol. 12, no. 1, pp. 176-179, 1967.
- [23] Al-Rawajfeh, A. E., CaCO₃-CO₂-H₂O system in falling film on a bank of horizontal tubes: Model verification, *Journal of Industrial and Engineering Chemistry*, vol. 16, no. 6, pp. 1050-1058, 2010.
- [24] Welch, P. D., The use of fast Fourier transform for the estimation of power spectra: A method based on time averaging over short, modified periodograms, *IEEE Transactions on Audio and Electroacoustics*, vol. 15, no. 2, pp. 70-73, 1967.
- [25] Krömer, K., Will, S., Loisel, K., Nied, S., Detering, J., Kempter, A., and Glade, H., Scale formation and mitigation of mixed salts in horizontal tube falling film evaporators for seawater desalination, *Heat Transfer Engineering*, vol. 36, no. 7-8, pp. 750-762, 2015.
- [26] D'Alessio, S. J. D., Pascal, J. P., Ellaban, E., and Ruyer-Quil, C., Marangoni instabilities associated with heated surfactant-laden falling films, *Journal of Fluid Mechanics*, vol. 887, 2020, Article A20, DOI: 10.1017/jfm.2019.1058.
- [27] Elfring, G. J., Leal, L. G., and Squires, T. M., Surface viscosity and Marangoni stresses at surfactant laden interfaces, *Journal of Fluid Mechanics*, vol. 792, pp. 712-739, 2016.
- [28] Lucassen-Reynders, E. H., and Lucassen, J., Surface dilational rheology: Past and present, In: *Interfacial rheology*, Eds. R. Miller and L. Liggieri, Brill, Leiden, Netherlands, 2009, pp. 38-76.
- [29] Desai, P. R., Jain, N. J., Sharma, R. K., and Bahadur, P., Effect of additives on the micellization of PEO/PPO/PEO block copolymer F127 in aqueous solution, *Colloids and Surfaces*, vol. 178, no. 1-3, pp. 57-69, 2001.
- [30] Green, R. J., Tasker, S., Davies, J., Davies, M. C., Roberts, C. J., and Tendler, S. J. B., Adsorption of PEO-PPO-PEO triblock copolymers at the solid/liquid interface: A surface plasmon resonance study, *Langmuir*, vol. 13, no. 24, pp. 6510-6515, 1997.
- [31] Oliveira, R., Understanding adhesion: A means for preventing fouling, *Experimental Thermal and Fluid Science*, vol. 14, no. 4, pp. 316-322, 1997.
- [32] Zettler, H. U., Weiß, M., Zhao, Q., and Müller-Steinhagen, H., Influence of surface properties and characteristics on fouling in plate heat exchangers, *Heat Transfer Engineering*, vol. 26, no. 2, pp. 3-17, 2005.